

## Supplementary Information

### **Role of Lewis acid-base pair sites on ZnO-ZnCr<sub>2</sub>O<sub>4</sub> catalyst for the cyclization by a dehydrogenative condensation of crude glycerol and 1,2-propanediamine for the synthesis of 2,6-dimethylpyrazine**

Krishna Vankudoth<sup>a,b</sup>, A. Hari Padmasri<sup>c</sup>, Reema Sarkari<sup>b</sup>, Vijay Kumar Velisoju<sup>b</sup>, Naresh Gutta<sup>b</sup>, Naveen Kumar Sathu<sup>b</sup>, C. N. Rohita<sup>b</sup> and Venugopal Akula<sup>a,b\*</sup>

<sup>a</sup>Academy of Scientific and Innovative Research, India

<sup>b</sup>Catalysis Laboratory, Inorganic and Physical Chemistry Division, CSIR-Indian Institute of Chemical Technology, Hyderabad, Telangana – 500007, India.

<sup>c</sup> Department of Chemistry, University College for Women, Osmania University, Koti, Hyderabad - 500 095, Telangana, India.

\*Corresponding author

#### **Abstract:**

Nano-crystalline mixed oxides of ZnO-ZnCr<sub>2</sub>O<sub>4</sub> (ZC) derived from Zn-Cr-HT precursors were examined for the vapor phase dehydrocyclization of crude glycerol and 1,2-propanediamine (1,2-PDA) to synthesize 2,6-dimethylpyrazine (1,2-DMP). Nature of surface active sites are illustrated by BET-SA, XRD, ESR, H<sub>2</sub>-TPR, TPD of NH<sub>3</sub>, TEM, XPS, pyridine and HCOOH adsorbed DRIFT spectroscopy. Role of acid-base sites on the product distribution is discussed using the catalytic activity data under kinetic regime. The in-situ IR studies revealed the dehydration of glycerol is occurring on weak Lewis acid and dehydrogenation is taking place on strong basic sites on the catalyst surface. A relationship between surface acid-base strength and the 2,6-DMP rate is established.

## 1.0 Preparation of Zn-Cr-O catalyst

The nano crystalline ZnO–ZnCr<sub>2</sub>O<sub>4</sub> mixed oxide sample was prepared by a simple co-precipitation method [1]. In a typical method required amounts of Zn(NO<sub>3</sub>)<sub>2</sub>·3H<sub>2</sub>O and Cr(NO<sub>3</sub>)<sub>3</sub>·9H<sub>2</sub>O were dissolved in double distilled water and the mixed salt precursors were co-precipitated by using a mixture of 2M NaOH + 1M Na<sub>2</sub>CO<sub>3</sub>, at various pHs (8, 10 and 12) under constant stirring. The resultant precipitate was washed several times with distilled water (until the pH reached ~ 8, 10, 12), filtered, dried in air at 120 °C over night. The oven dried sample showed the Zn-Cr hydrotalcite like structure with diffraction line at  $2\theta = 11.6^\circ$ ,  $23.5^\circ$  and  $34.57^\circ$  in the XRD (Figure S2). The dried Zn-Cr HT sample was calcined in static air at 500 °C with a heating rate of 10 °C min<sup>-1</sup>. The nano crystalline ZnO-ZnCr<sub>2</sub>O<sub>4</sub> mixed oxides synthesized at different pH are denoted as ZC8, ZC10 and ZC12 respectively. For comparison purpose both the bulk Zinc oxide (ZnO) and chromium oxide (Cr<sub>2</sub>O<sub>3</sub>) were prepared using their respective nitrate salts under similar protocol.

## 1.1 Characterization of catalysts

The bulk and surface properties of the samples were analysed by BET-surface area, powder X-ray diffraction (XRD), Transmission electron microscopy (TEM), Fourier transform infrared (FT-IR), Temperature programmed reduction (H<sub>2</sub>-TPR), X-ray photoelectron spectroscopy (XPS), carbon-hydrogen-nitrogen-sulphur (CHNS) analyses and Temperature programmed desorption of NH<sub>3</sub> (NH<sub>3</sub>-TPD) techniques. To investigate the nature and strength of acid-base sites; pyridine and formic acid adsorbed FT-IR (Carry 660, Agilent Technologies) spectra were recorded at a resolution of 4 cm<sup>-1</sup>. The experiments were performed in-situ using a purpose made IR cell connected to a conventional vacuum adsorption apparatus. In a typical method the sample powder was pressed into self-supporting wafers (density ~40 mg cm<sup>-2</sup>) under a pressure of 10<sup>5</sup> Pa. After that, the sample was introduced in the IR cell. Firstly, the sample was pre-treated *in-situ* by heating in dynamic

vacuum at a rate of 10 °C min<sup>-1</sup> up to 450 °C for 1 h. After cooling down to 150 °C, the spectrum (fresh) was collected in the DRIFT mode. Prior to pyridine adsorption, the self supporting wafers were reduced using 5% H<sub>2</sub> balance Ar at 400 °C for 30 min and cooled to 150 °C in N<sub>2</sub> flow. Then the pyridine vapour was injected onto the sample in 3 successive pulses (with a total of ~6 µL) followed by flushing the sample in N<sub>2</sub> for 1 h and the spectrum was recorded. The pyridine adsorbed DRIFT spectrum was subtracted with that of reduced sample spectrum to obtain the vibrational bands due to pyridine-acid (Brønsted acid site: Py-H<sup>+</sup> and Lewis acid site: Py-M<sup>n+</sup>) site interaction. In a similar protocol the formic acid adsorbed (a dose of 6 µL) and H<sub>2</sub>O (6 µL) adsorbed DRIFT spectra were collected in separate measurements. Finally, the spectra were quantified with Kubelka-Munk function. The elemental analysis of the samples revealed that there is no loss of metal during the preparation and activation (Table S1).

## 1.2 Product analysis

The vapour phase dehydrocyclization of aqueous glycerol in conjunction with and 1,2-PDA was carried out in a fixed bed down flow quartz reactor at atmospheric pressure at 375 °C independently, under kinetic regime (Glycerol:1,2-PDA:H<sub>2</sub>O:N<sub>2</sub> = 1:1: 26.3:20.4). The samples were analyzed by gas chromatograph (Shimadzu, GC-17A) via a flame ionization detector (FID) using a ZB-5 capillary column at a ramping rate of 10 °C min<sup>-1</sup> from 60 to 280 °C. The carbon mass balance for all the measurements was > 95%. The samples were analyzed by GC-MS (QP5050A Shimadzu) using a ZB-5 capillary column with EI mode.

**2,6-dimethylpyrazine:** M<sup>+</sup> m/z: 108; (M-CH<sub>3</sub>)<sup>+</sup> m/z: 93; (M-HCN)<sup>+</sup> m/z: 81; (M-C<sub>3</sub>H<sub>6</sub>)<sup>+</sup> m/z: 66; [M-C<sub>3</sub>H<sub>2</sub>N<sub>2</sub>]<sup>+</sup> m/z: 42; **Dihydroxyacetone:** M<sup>+</sup> m/z: 90; [M-H<sub>2</sub>O]<sup>+</sup> m/z: 72; [M-CH<sub>2</sub>O]<sup>+</sup> m/z: 60; [M-(CO, H<sub>2</sub>O)]<sup>+</sup> m/z: 43; [M-(CO, CH<sub>2</sub>CH<sub>2</sub>)]<sup>+</sup> m/z: 31; [M-C<sub>3</sub>H<sub>4</sub>O<sub>2</sub>]<sup>+</sup> m/z: 18; **Hydroxyacetone:** M<sup>+</sup> m/z: 74; [M-CH<sub>2</sub>O]<sup>+</sup> m/z: 43; [M-(CO, CH<sub>3</sub>)]<sup>+</sup> m/z: 31; [M-

$C_2H_3O_2]^+$  m/z: 15; **6-hydroxymethyl-2-methylpyrazine**:  $M^+$  m/z: 124;  $(M-H)^+$  m/z: 123;  
 $(M-CH_2O)^+$  m/z: 94;  $(M-CH_3CN)^+$  m/z: 83;  $(M-C_3H_2N_2O)^+$  m/z: 42.

### 1.3 Calculations of conversion, rate and specific rate:

$$\%Conversion\ of\ 1,2 - PDA = \left[ \frac{moles_{1,2 - PDA\ in} - moles_{1,2 - PDA\ out}}{moles_{1,2 - PDA\ in}} \right] \times 100$$

$$\%Conversion\ of\ Glycerol = \left[ \frac{moles_{Gly.\ in} - moles_{Gly.\ out}}{moles_{Gly.\ in}} \right] \times 100$$

$$\%Selectivity = \left[ \frac{P_i / C_i}{\sum_i^n P_i / C_i} \right] \times 100$$

(where  $C_i$  and  $P_i$  are the stoichiometric factor and the product concentration, respectively).

$$Yield_{2,6 - DMP} = \frac{[Conv_{Gly.} \times Sel_{2,6 - DMP}]}{100}$$

$$Yield_{6 - HMP} = \frac{[Conv_{Gly.} \times Sel_{6 - HMP}]}{100}$$

Rate ( $r$ ) is defined as

$$r_{2,6 - DMP} = \left[ \frac{(Yield_{2,6 - DMP}) \times (1,2 - PDA + Glycerol)\ flow\ rate}{Weight\ of\ the\ catalyst} \right] moles\ g_{cat}^{-1}\ s^{-1}$$

$$r_{6 - HMP} = \left[ \frac{(Yield_{6 - HMP}) \times (1,2 - PDA + Glycerol)\ flow\ rate}{Weight\ of\ the\ catalyst} \right] moles\ g_{cat}^{-1}\ s^{-1}$$

## 1.4 DTA-TGA

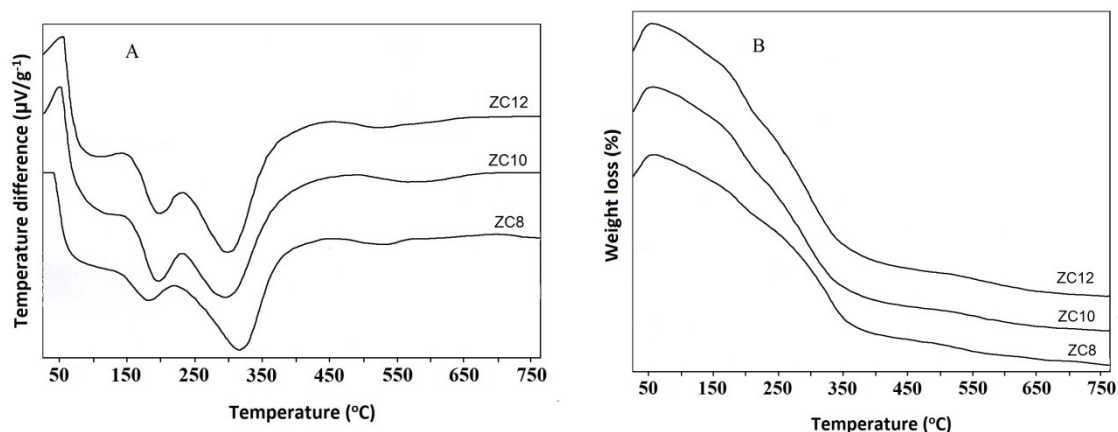


**Figure S1:** (A) DTA (B) TGA analysis of oven dried Zn-Cr-O samples.

Hydroxalcalite-type materials decompose in three consecutive steps resulting in plateaus in the TGA diagram and endothermic peaks in the DTA pattern. There are three endothermic peaks in DTA pattern of Zn-Cr-O samples prepared at different pH levels (8, 10 and 12) located at around 110  $^{\circ}\text{C}$ , 200  $^{\circ}\text{C}$  and 320  $^{\circ}\text{C}$ . The DTA weak and broad endothermic peak observed between 80 to 127  $^{\circ}\text{C}$ , which is due to removal of weakly adsorbed water molecules, probably on the external surface of the particles. The endothermic peak observed between 200 to 250  $^{\circ}\text{C}$ , which is due to removal of water of crystallization accompanied with dehydroxylation of the hydroxy groups from brucite like layered structure. The endothermic peak at 320 to 450  $^{\circ}\text{C}$ , this is ascribed to the removal of carbon dioxide from the interlayer carbonate anion. Further weight loss beyond 450  $^{\circ}\text{C}$  is not seen, indicating that decomposition did not occur above 450  $^{\circ}\text{C}$  temperature. From these it can be inferred that Zn-Cr-O mixed oxides are thermally stable at 450  $^{\circ}\text{C}$ .

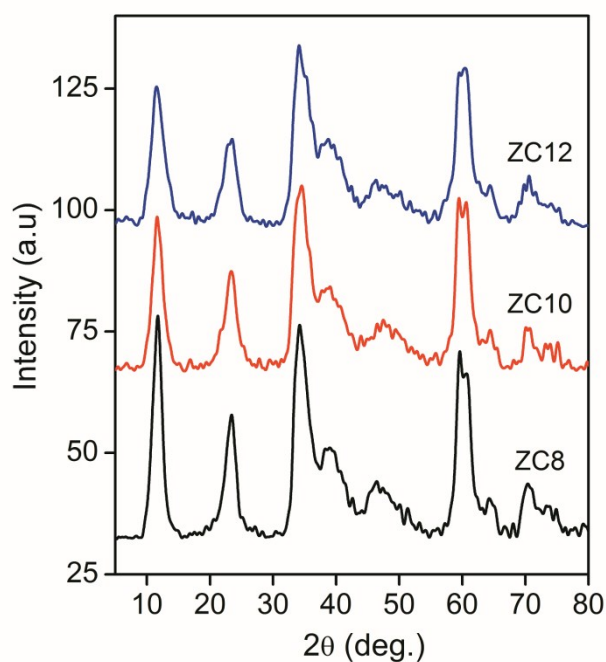


**Figure S2:** XRD pattern of oven dried Zn-Cr-O samples

The hydroxaltes are layered double hydroxides (LDHs) which have the general molecular formula  $M^{2+}_{1-x}M^{3+}_x(OH)_2(A^{n-})_{x/n} \cdot mH_2O$ , where  $M^{2+}$  and  $M^{3+}$  are a divalent and a trivalent metal cations that occupy octahedral positions in brucite-like layers, respectively, and  $A^{n-}$  is an interlayer anion. Structurally, they possess brucite-like ( $Zn(OH)_2$ ) sheets where isomorphous substitution of  $Zn^{2+}$  by a trivalent cation like  $Cr^{3+}$  occurs.  $M$  the number of interlayer water molecules and  $x$  the atomic ratio  $M^{3+}/(M^{2+}+M^{3+})$  [1]. The resulting excess of positive charge in the layered network is compensated by anions, which occupy the interlayer space along with water molecules. By controlled thermal decomposition, LDHs are converted into mixed oxides.

## 1.5 FTIR Analysis

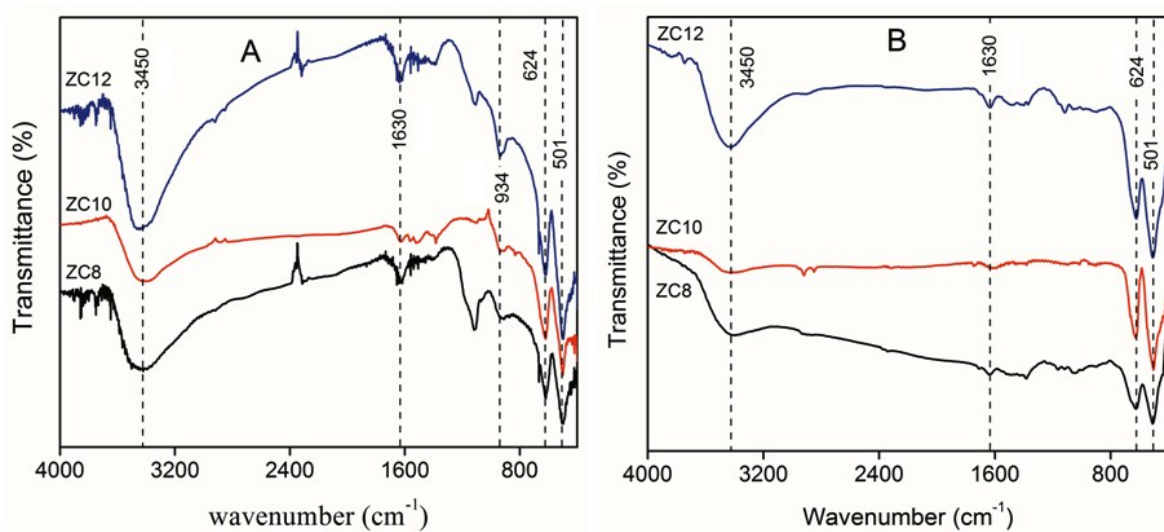


Figure S3: FT-IR spectra of (A) calcined and (B) reduced Zn-Cr-O samples.

## 1.6 TPD of NH<sub>3</sub>

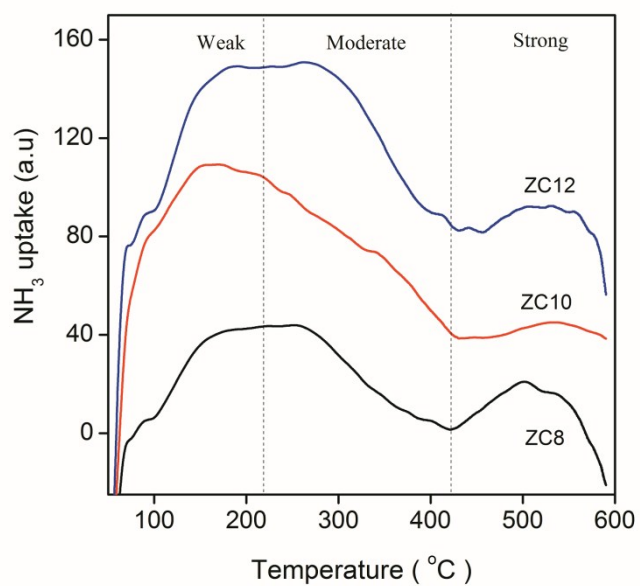


Figure S4: TPD pattern of Zn-Cr-O samples.

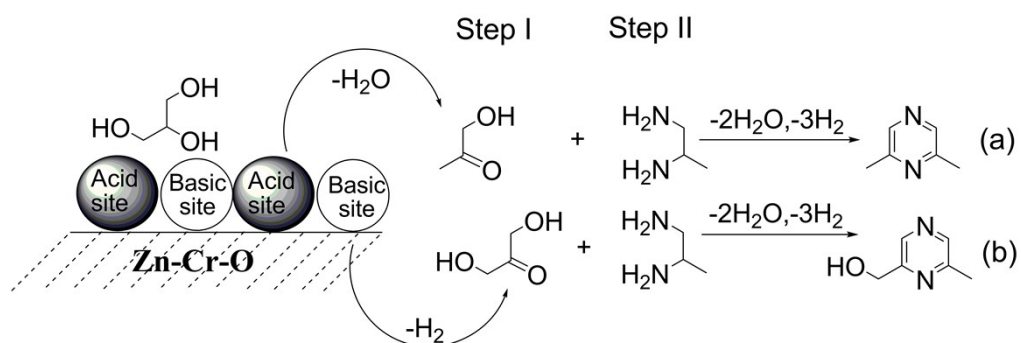
Table S1: Elemental analysis by atomic absorption spectroscopy

Sample	Nominal composition (Zn:Cr) mole ratio	AAS composition (Zn:Cr) mole ratio	
		Calcined	Spent
ZC8	2.0:1.0	1.95:0.97 = 2.01	1.92:0.96 = 2.0
ZC10	2.0:1.0	1.98:0.96 = 2.06	1.96:0.95 = 2.06
ZC12	2.0:1.0	1.97:1.03 = 1.91	1.98:0.98 = 2.02

Table S2: Time on stream analysis on ZC10 sample at 375 °C; GHSV at 7.36 mL g<sub>cat</sub><sup>-1</sup> s<sup>-1</sup>.

Time (h)	Conversion (%)		Selectivity (%)			
	$X_{\text{glycerol}}$	$X_{1,2\text{-PDA}}$	$S_{2,6\text{-DMP}}$	$S_{6\text{-HMP}}$	$S_{2,6\text{-DMPip}}$	$^a S_{\text{others}}$
1	19.8	20.8	68.5	13.6	8.6	9.3
2	20.5	21.7	68.3	12.6	8.4	10.7
2	20.2	21.6	68.0	12.5	8.4	11.1
4	20.0	20.7	67.5	10.5	8.1	13.9
5	18.5	20.1	67.2	10.3	7.4	15.1
5	17.2	19.3	65.4	10.1	7.3	17.2
7	17.2	18.7	65.2	9.7	6.9	18.2
8	16.3	17.6	65.2	9.8	6.8	18.2
9	15.4	15.8	65.0	9.8	6.5	18.7
10	15.0	15.6	65.0	9.1	6.5	19.4
11	13.7	15.1	64.6	8.7	5.2	20.5
12	12.2	12.8	64.3	8.5	5.3	21.9
13	12.2	12.7	64.4	8.5	5.4	21.7
14	11.6	12.4	63.8	8.3	5.2	22.7
15	10.4	11.1	63.3	8.3	5.1	23.3

<sup>a</sup> Others include 2,5-DMP and 5-HMP.



Scheme S1: Cyclization by a dehydrogenative condensation of glycerol and 1,2-propanediamine on acid-base sites of Zn-Cr-O catalysts

## References

1. A. Venugopal, S. Reema, Ch. Anjaneyulu, V. Krishna and M. K. Kumar, *Appl. Catal. A: Gen.* 2012, **441–442**, 108–118.
2. M. A. Pagano, C. Forano and J.P. Besse, *J. Mater. Chem.*, 2003, **13**, 1988–1993.